

# A conditionally invariant mathematical morphological framework for color images



Tao Lei<sup>a,b,\*</sup>, Yanning Zhang<sup>b</sup>, Yi Wang<sup>c</sup>, Shigang Liu<sup>d</sup>, Zhe Guo<sup>c</sup>

<sup>a</sup> College of Electronical and Information Engineering, Shaanxi University of Science & Technology, Xi'an 710021, China

<sup>b</sup> School of Computer Science, Northwestern Polytechnical University, Xi'an 710072, China

<sup>c</sup> School of Electronics and Information, Northwestern Polytechnical University, Xi'an 710072, China

<sup>d</sup> School of Computer Science, Shaanxi Normal University, Xi'an 710119, China

## ARTICLE INFO

### Article history:

Received 23 June 2015

Revised 10 December 2016

Accepted 1 January 2017

Available online 5 January 2017

### Keywords:

Mathematical morphology

Color image processing

Duality

Vector ordering

## ABSTRACT

It is difficult to extend a grayscale morphological approach to color images because total vector ordering is required for color pixels. To address this issue, we developed a kind of vector ordering method based on linear transformations from RGB to other color spaces (i.e., YUV, YIQ and YCbCr) and principal component analysis (PCA). Additionally, we propose a conditionally invariant morphological framework based on the proposed vector ordering. We also define elementary multivariate morphological operators (e.g., multivariate erosion, dilation, opening and closing), and investigate their properties with a focus on duality. The proposed framework guarantees some important properties of classical mathematical morphology, such as translation-invariance, conditional increasingness, and duality. Therefore, it is easy to extend existing grayscale morphological approaches to color images in terms of the proposed multivariate morphological framework (MMF). Simulation results show the potential abilities of MMF in color image processing, such as image filtering, reconstruction, and segmentation.

© 2017 Elsevier Inc. All rights reserved.

## 1. Introduction

Mathematical morphology founded by Matheron and Serra [39], is a nonlinear image processing methodology based on the application of lattice theory to spatial structures [11]. It is an important technological component commonly implemented in a variety of research fields, such as image processing, pattern recognition, and computer vision [6,13,36]. Compared with grayscale images, color images provide richer information. Accordingly, the research dedicated to extending mathematical morphological approaches from grayscale images to color images has attracted considerable interest in recent years [2,14,21,26,38]. However, this extension is not straightforward because of the vectorial nature of color data [18]. According to classical mathematical morphology, the concept of a supremum (or infimum) of colorized pixels is necessary for the extension since color pixels must be described by three separate values (RGB) as opposed to a single grayscale value. Consequently, it is crucial to define a total vector ordering which always causes important irregularities [14], before achieving the extension [1,19]. Unlike scalars, there is no unambiguous way of ordering vectors for color data. At present, several approaches applied to vector ordering of color data have been reported and can be classified into roughly four categories [7,22,24,41]: marginal ordering, conditional ordering, reduced ordering, and partial ordering. Marginal ordering is easy to

\* Corresponding author.

E-mail address: [leitaoly@163.com](mailto:leitaoly@163.com) (T. Lei).

be implemented, but often suffers from a “false color” problem [21]. An example of conditional ordering, lexicographical ordering, has been widely employed in multivariate morphology approaches. As HSV color space is the way human beings inherently perceive color, lexicographical ordering, which is based on brightness, saturation and hue components, was proposed in previous studies [35,41]. Recently, Angulo [4] applied quaternion decomposition to color image representation and then proposed a new lexicographical ordering that provided better results than traditional approaches. This reduced ordering is easy in implementation and has lower computational complexity. Considering that RGB color space is widely used in electronic devices for capturing and displaying images in computational systems, Witte et al. [16] defined a vector ordering based on Euclidean distance in RGB color space, and proposed the definitions and applications of multivariate morphological operators (MMOs). In addition, the combination of different multivariate distances and lexicographical orderings is also very popular in multivariate mathematical morphology (MMM). Motivated by this, Angulo [3] introduced a generalization of distance-based and lexicographical-based approaches. Lei et al. [30] further proposed a novel multivariate morphological approach by defining vector ordering in HSV color space. Other research on fuzzy lexicographical ordering models has also been conducted [8,9,34].

In addition to the aforementioned vector ordering approaches, partition ordering is another, though non-mainstream, method. Few schemes [42,43,45] applying partition ordering to multivariate morphological framework (MMF) have been reported. However, partition ordering has developed rapidly in recent years. Velasco-Forero et al. [43] proposed a mathematical morphological approach based on a statistical depth function. Furthermore, the kriging-based supervised ordering has been introduced and used to define MMOs [42,45]. More recently, various complex mathematical tools, such as learning algorithms [37,44], principal component analysis (PCA) [31], probabilistic extrema estimation [12], quaternions [5,29], and group-invariant frames [20], have been employed by MMM to improve the performance of MMOs for color image processing.

Although a number of multivariate morphological approaches have been introduced and applied to multi-channel images [15,32,33], few studies have been conducted on their relevant properties, e.g., duality. To extend grayscale morphological algorithms to color image processing, we propose in this paper a conditionally invariant morphological framework based on different color spaces (i.e., YUV, YIQ and YCbCr) and a PCA transformation. Our primary contributions include the following:

- (1) Demonstrating that transformations from RGB to other color spaces (including YUV, YIQ, and YcbCr) are more suitable for constructing MMOs with duality than transformations from RGB to color spaces (including HSV, HLS, HIS, and CIELAB).
- (2) Proposing a vector ordering method that is based on linear transformations of RGB and PCA.
- (3) Conducting experiments that demonstrate that the proposed MMOs satisfy duality. Moreover, it is easy to extend grayscale morphological algorithms to our MMF.

This paper is organized as follows: In [Section 2](#), we provide the motivation for our work. In [Section 3](#), we analyze the duality of MMOs and provide the necessary conditions for the construction of dual multivariate operators. In [Section 4](#), we propose a new vector-ordering principle based on linear transformations of RGB color space and employ it to construct MMOs. [Section 5](#) suggests various applications, including color image filtering, reconstruction, and segmentation. Finally, we present our conclusions in [Section 6](#).

## 2. Motivation

### 2.1. Duality of grayscale mathematical morphology

Duality, a property allowing one operation to be expressed in terms of another, is one of the most important principles in mathematical morphology. In classical mathematical morphology, most operators occur in pairs of dual operators, such as erosion and dilation, or opening and closing [28,40]. Such operators do not necessarily need to exist as opposites of each other. Moreover, some complex morphological transformations are also proposed in terms of dual operators, such as morphological gradient operators, reconstruction operators, the top-hat transformation, and self-dual morphological operators. Consequently, duality is an important factor for extending elementary morphological operators to color images. In the following, we first review some elementary concepts of mathematical morphology.

**Definition 1.** The complement of a grayscale image  $f$ , denoted by  $f^c$ , is defined for each pixel  $\mathbf{x}$  as the maximum value  $t_{\max}$  (e.g.,  $t_{\max} = 255$  for an 8-bit grayscale image) of the unsigned data type used for storing the image minus the value of the image  $f$  at position  $\mathbf{x}$ ,

$$f^c(\mathbf{x}) = t_{\max} - f(\mathbf{x}). \quad (1)$$

**Definition 2.** The complement image of a color image  $\mathbf{f}$ ,  $\mathbf{f} \in (E, T^{RGB})$ , is defined as the complement of each color component [3], i.e.,

$$\mathbf{f}^c = (r^c, g^c, b^c) = (t_{\max} - r + t_{\min}, t_{\max} - g + t_{\min}, t_{\max} - b + t_{\min}). \quad (2)$$

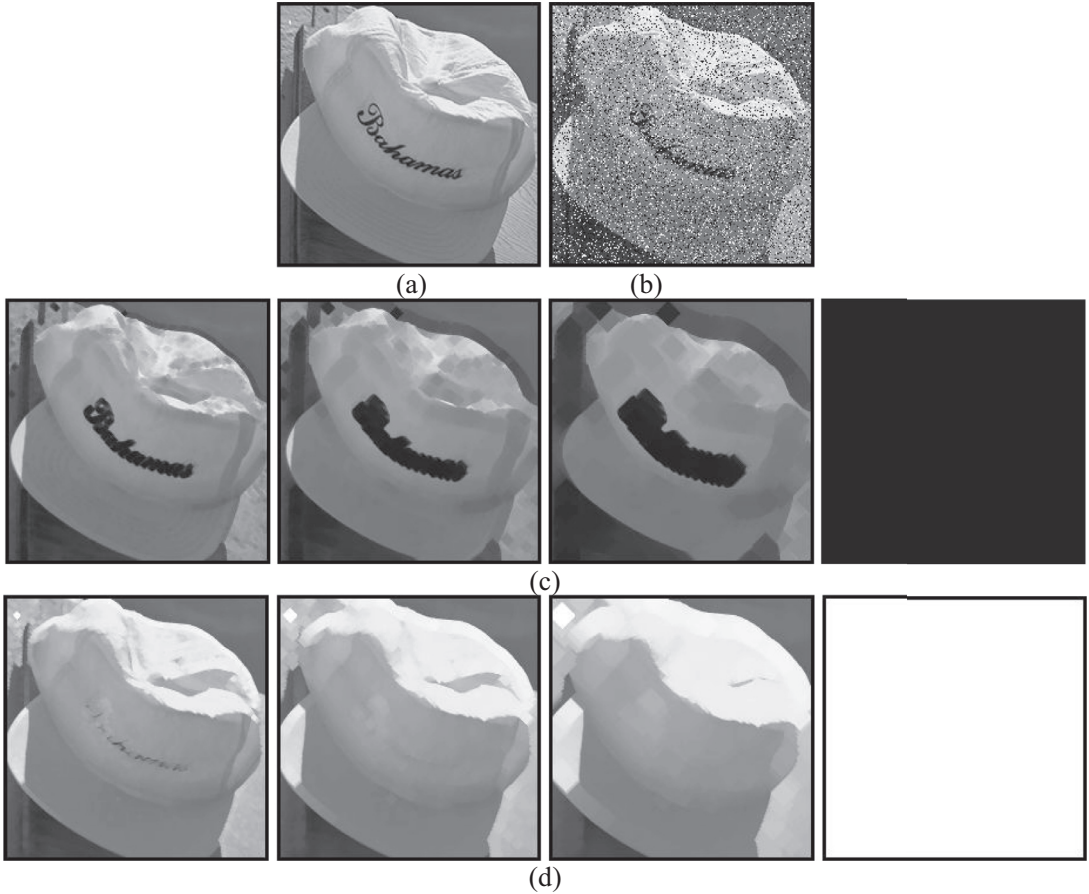


**Fig. 1.** Results using iterative dual operators ( $\varepsilon, \delta$ ). (a) Original gray image “Cap”. (b) “Cap” containing 20% salt & pepper noise. (c) Iterative erosion (from left to right  $\varepsilon^3, \varepsilon^5, \varepsilon^{220}$ ). (d) Iterative dilation (from left to right  $\delta, \delta^3, \delta^5, \delta^{220}$ ).

**Definition 3.** Any two image transformations  $\psi$  and  $\psi'$  are dual with respect to complementation if applying  $\psi$  to an image is equivalent to applying  $\psi'$  to the complement of the image and then complementing the resulting image,

$$\psi(f/\mathbf{f}) = (\psi'(f^c/\mathbf{f}^c))^c. \quad (3)$$

In general, given the dual operator  $\psi$ , we denote its dual operator by  $\psi^*$ . That is,  $\psi^* = \psi'$  and  $(\psi')^* = \psi$ . Likewise,  $\gamma^* = \varphi$  and  $\varphi^* = \gamma$ , while  $\varepsilon^* = \delta$  and  $\delta^* = \varepsilon$  ( $\varepsilon$  and  $\delta$  denote erosion and dilation, respectively, while  $\gamma$  and  $\varphi$  denote opening and closing, respectively).

Generally, the erosion operation removes bright image structures, while the dilation operation has the same effect on dark image structures. Hence, the composition operators of morphological erosion and dilation are usually used to remove noise in images. Fig. 1 shows various images filtered by dual morphological operators.

Fig. 1 illustrates that the images produced by the erosion operation become brighter, while the images produced by the dilation operation become darker. By iterative operations, the original image turns into a pure image with a single minimum or maximum grayscale value. Therefore, a unique supremum and infimum exists for grayscale images. In addition, the morphological combination operators (e.g., opening, closing, opening-closing and closing-opening) are employed to suppress noise. Fig. 2 shows various images filtered by dual morphological operators.

Different results are provided by  $(\gamma, \varphi)$  and  $(\varphi\gamma, \gamma\varphi)$  in Fig. 2. Although filters  $\gamma$  and  $\varphi\gamma$ , the first of which is the erosion operation, are able to remove bright image structures and some dark structures, the filtered images still contain some dark noise structures. Similarly,  $\varphi$  and  $\gamma\varphi$  preserve some of the bright noise structures. Clearly, a pair of dual morphological operators results in different filtering effects but approximately the same peak signal-to-noise ratio (PSNR). For instance,  $\gamma$  has PSNR approximately that of  $\varphi$ .

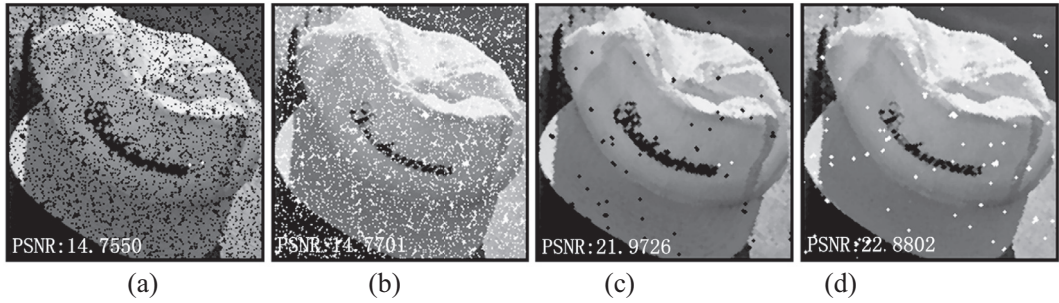


**Fig. 2.** Images filtered by dual morphological filters. (a) Opening (PSNR = 14.755). (b) Closing (PSNR = 14.7701). (c) Opening-closing (PSNR = 21.9726). (d) Closing-opening (PSNR = 22.8802).

**Table 1**  
Popular vector orderings.

Vector ordering	Reference
VSH (Value-Saturation-Hue, $\leq_{Louverdis}$ )	[35]
DLSH (Distance-Luminance-Saturation-Hue, $\leq_{Angulo07}$ )	[3]
QPEPA (Quaternion decomposition, Perpendicular-Parallel, $\leq_{Angulo10}$ )	[4]
HVSD (Hybrid Value and Saturation Distance in the HSV color space, $\leq_{Lei13}$ )	[30]
FEEA (Fuzzy Extremum Estimation Algorithm, $\leq_{Lei14}$ )	[29]

## 2.2. MMO duality

As described in [Section 2.1](#), a morphological filter has a similar effect for noise removal as its dual operator. By extending this duality to multivariate mathematical morphology, we conclude that dual multivariate morphological filtering operators, such as multivariate opening and closing, achieve a similar effect for noise removal in color images. The color image “Cap”, corrupted by impulse noise, is filtered by MMOs using the five popular vector orderings, listed in [Table 1](#). The results are shown in [Fig. 3](#) ( $\vec{\gamma}$  and  $\vec{\phi}$  represent multivariate opening and closing, respectively).

[Fig. 3](#) demonstrates that multivariate morphological opening is able to suppress noise, while multivariate morphological closing enhances this noise. Thus, existing multivariate morphological filtering operators, which begin with multivariate dilation, provide poor results for noise removal.

From [Fig. 3](#), we conclude that, due to duality, it is difficult to extend the applications of multivariate morphological approaches [3,4,29,30,35] in color image processing. In fact, Angulo [3] found the problem of duality for MMOs in a prior study. He showed that duality is always valid for orderings grounded exclusively in lexicographical cascades, without including pre-ordering based on the distance to a reference. Moreover, he demonstrated that no property of duality seems to be associated with the complement of a reference color. However, it is unclear why multivariate openings provide better filtering results than multivariate closings ([Fig. 3](#)). Below, we propose some possible reasons for this observation.

Morphological dilation and erosion are inconsistent and might introduce aliasing at boundaries [14]. An illustration of this problem is given in the following example.

The HSV color space is popular for defining MMMs, such as VSH [35] and HVSD [30]. HSV color model is an asymmetric cone, as shown in [Fig. 4](#). Only a unique black pixel with minimal brightness ( $v=0$ ) is obtained after iterating the erosion operation. An arbitrary pixel with maximal brightness ( $v=1$ ) and a fixed normalized saturation value (ranging from 0 to 1) will be obtained after iterating the dilation operation. As a result, multivariate morphological erosion results are convergent, while dilation is divergent. Accordingly, the asymmetry of the HSV color space is an important factor leading to order irregularities, which produces worse results for closing than opening. The total order provided by DLSH, QPEPA, and FEEA also leads to irregularity issues.

If we apply VSH, DLSH, QPEPA, HVSD and FEEA to color pixel orderings, we find that erosion is efficient for vector ordering, but dilation is inefficient. These results are shown in [Fig. 5](#), which demonstrates the vector ordering is consistent with HSV color space, and that the minimal color pixel tends to be black, while the maximal color pixel does not tend to be white. It is obvious that the order among large color pixels is irregular due to the disordering of the hue component (see the right red rectangle in [Fig. 5b](#)), which is an irregularity issue caused by the total orders. This is the reason why multivariate closing provides worse results than multivariate opening (see [Fig. 3](#)).

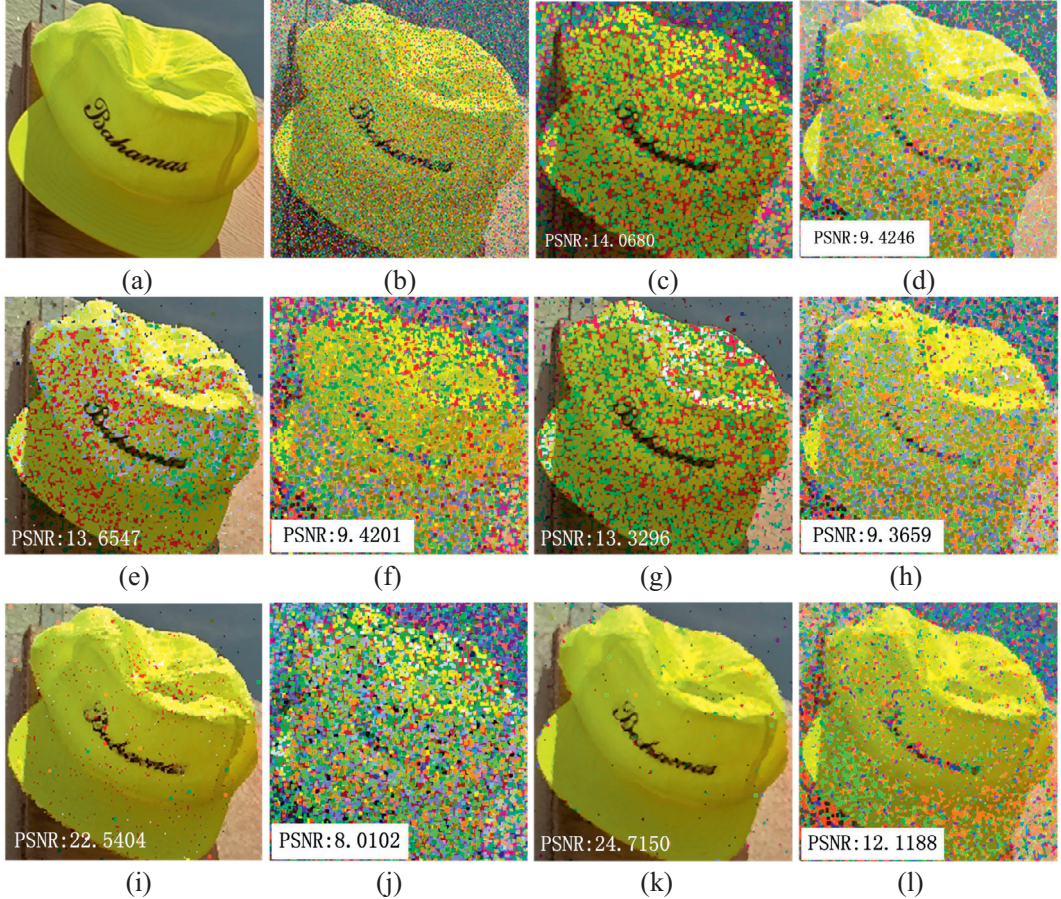


**Fig. 3.** Restoration results from different multivariate morphological filters for image “Cap” corrupted by 20% impulse noise. (a) Original image “Cap”. (b) “Cap” containing 20% salt & pepper noise. (c)  $\vec{\gamma}_{VSH}$ . (d)  $\vec{\phi}_{VSH}$ . (e)  $\vec{\gamma}_{DLSH}$ . (f)  $\vec{\phi}_{DLSH}$ . (g)  $\vec{\gamma}_{QPEPA}$ . (h)  $\vec{\phi}_{QPEPA}$ . (i)  $\vec{\gamma}_{HVSD}$ . (j)  $\vec{\phi}_{HVSD}$ . (k)  $\vec{\gamma}_{FEEA}$ . (l)  $\vec{\phi}_{FEEA}$ .

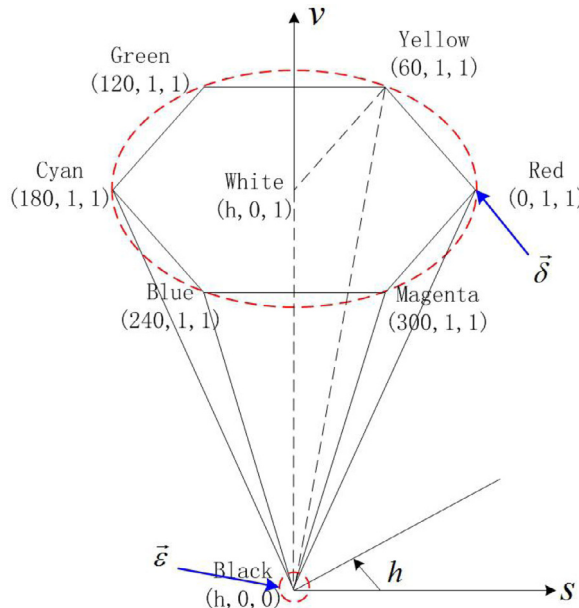


**Fig. 4.** HSV color model.

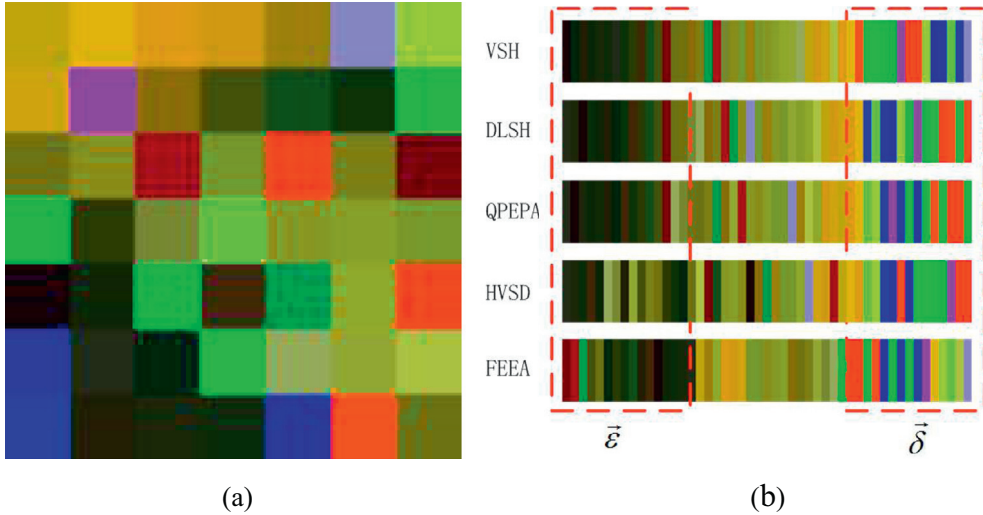


**Fig. 5.** Sorting results of color pixels (a) A  $7 \times 7$  color block. (b) Ordering results of color pixels.

### 3. MMF

#### 3.1. Concepts

Before introducing MMM, we first recall some basic notions of classical mathematical morphology theory. A set  $\mathcal{L}$  with a partial ordering  $\leq$  is called a complete lattice if every subset  $\mathcal{H}$  of  $\mathcal{L}$  has a lowest upper bound (supremum)  $\vee \mathcal{H}$  and a greatest lower bound (infimum)  $\wedge \mathcal{H}$ . Letting  $E$  and  $\mathcal{T}$  represent nonempty sets, we denote  $\mathcal{F}(E, \mathcal{T})$  by the power set  $T^E$ , i.e., the functions mapping from  $E$  into  $\mathcal{T}$ . If  $\mathcal{T}$  is a complete lattice, then  $\mathcal{F}(E, \mathcal{T})$  is also a complete lattice. The operator  $\psi: E \rightarrow \mathcal{T}$  theory is increasing if  $\forall f, g \in \mathcal{F}(E, \mathcal{T})$ , and  $f \leq g \Rightarrow \psi(f) \leq \psi(g)$ .  $\psi$  is extensive if  $f \leq \psi(f)$ , and is anti-extensive if  $\psi(f) \leq f$ . The operator  $\psi: \mathcal{T} \rightarrow \mathcal{T}$  theory is called an operator on  $\mathcal{T}$ . The simplest operator on  $\mathcal{T}$  is the identity operator, which maps every element into itself and is denoted by *id*.  $id(f) = f$ , for  $\forall f \in \mathcal{T}$ . An operator is idempotent if  $\psi(\psi(f)) = \psi(f)$ . It is dilation if  $\psi(\bigvee_{t \in b} f_{-t}) = \bigvee_{t \in b} \psi(f_{-t})$ , where  $b$  theory is a structuring element. Duality is erosion if  $\psi(\bigwedge_{t \in b} f_{-t}) = \bigwedge_{t \in b} \psi(f_{-t})$ .

If  $\varepsilon: E \rightarrow \mathcal{T}$  theory and  $\delta: \mathcal{T} \rightarrow E$  are two operators, we define the pair  $(\varepsilon, \delta)$  as an adjunction between  $\mathcal{T}$  and  $E$  if  $\delta(g) \leq f \Leftrightarrow g \leq \varepsilon(f)$ ,  $\forall f, g \in \mathcal{F}(E, \mathcal{T})$ . If  $(\varepsilon, \delta)$  is an adjunction, then  $\varepsilon$  is an erosion and  $\delta$  is a dilation. For every erosion  $\varepsilon: E \rightarrow \mathcal{T}$ , there corresponds a unique dilation  $\delta: \mathcal{T} \rightarrow E$  theory such that  $(\varepsilon, \delta)$  is an adjunction. Similarly, for every dilation  $\delta$ , one can associate a unique erosion  $\varepsilon$ . We then say that  $\varepsilon$  and  $\delta$  are adjoined to each other. According to the definition of  $\varepsilon$  and  $\delta$ ,  $\varepsilon \leq id$  theory and  $id \leq \delta$ .  $\delta\varepsilon$  and  $\varepsilon\delta$  are the compositions of  $\varepsilon$  and  $\delta$ , which form an opening on  $E$  and a closing on  $\mathcal{T}$ , respectively. An opening operator is increasing, anti-extensive, and idempotent; a closing operator is increasing, extensive, and idempotent. With every complete lattice  $\mathcal{T}$ , one can associate an opposite or dual complete lattice  $\mathcal{T}'$  by reversing the partial ordering:  $f \leq' g$  in  $\mathcal{T}'$  theory if  $g \leq f$  theory in  $\mathcal{T}$ . This observation forms the basis of the duality principle, which states that every definition or statement concerning complete lattices has a dual counterpart. For example, the dual of opening is closing, and vice versa.

#### 3.2. Ordering relations

Partial ordering plays a key role in mathematical morphology since output values at a given pixel for fundamental operators require that the ordering of input image values falls within a user-defined neighborhood centered at this pixel. Typically, a set of grayscale values in their natural order forms a completely-ordered set, and the maximum and minimum values for the set are uniquely defined. However, when there is no unambiguous means of defining the minimum and maximum values between two vectors in more than one dimension, the lack of a total ordering can only be partially answered by considering a suitable (less than total) sub-ordering. Therefore, a well-defined total ordering is necessary for MMOs. Two examples are presented in the following.

**Example 1.** Louverdis et al. [35] proposed a new color morphological operator in HSV color space. The vector ordering  $\leq_{Louverdis}$  of two pixels  $x_1(h_1, s_1, v_1)$  and  $x_2(h_2, s_2, v_2)$  is defined as follows:

$$x_1(h_1, s_1, v_1) \leq_{Louverdis} x_2(h_2, s_2, v_2) \Leftrightarrow \begin{cases} v_1 < v_2 \text{ or} \\ v_1 = v_2 \text{ and } s_1 \geq s_2 \text{ or} \\ v_1 = v_2 \text{ and } s_1 = s_2 \text{ and } h_1 \leq h_2 \end{cases} .$$

Based on the vector ordering  $\leq_{Louverdis}$ , Louverdis proposed the corresponding color erosion and dilation, which are denoted by  $\vec{\epsilon}_{Louverdis}$  and  $\vec{\delta}_{Louverdis}$ , respectively. They have some properties, such as translation-invariance and increasingness, but they do not satisfy duality.

**Definition 4.** The multivariate morphological erosion is given by

$$\vec{\epsilon}_b(\mathbf{f})(\mathbf{x}) = \wedge_{\substack{\mathbf{y} \\ \mathbf{y} \in b}} \{ \mathbf{f}(\mathbf{x} + \mathbf{y}) \}. \quad (4)$$

**Definition 5.** The multivariate morphological dilation is given by

$$\vec{\delta}_b(\mathbf{f})(\mathbf{x}) = \vee_{\substack{\mathbf{y} \\ \mathbf{y} \in b}} \{ \mathbf{f}(\mathbf{x} - \mathbf{y}) \}. \quad (5)$$

VO denotes the corresponding vector ordering.  $\vec{\epsilon}_{Louverdis}$  and  $\vec{\delta}_{Louverdis}$  are defined as

$$(\vec{\epsilon}_{Louverdis})_b(\mathbf{f})(\mathbf{x}) = \wedge_{\substack{\mathbf{y} \\ \mathbf{y} \in b}} \{ \mathbf{f}(\mathbf{x} + \mathbf{y}) \}, \text{ and} \quad (6)$$

$$(\vec{\delta}_{Louverdis})_b(\mathbf{f})(\mathbf{x}) = \vee_{\substack{\mathbf{y} \\ \mathbf{y} \in b}} \{ \mathbf{f}(\mathbf{x} - \mathbf{y}) \}, \quad (7)$$

where  $\mathbf{f}$  denotes a color image, and  $b$  is a structuring element.

To prove the duality of  $(\vec{\epsilon}_{Louverdis}, \vec{\delta}_{Louverdis})$ , we let  $\mathbf{f} = (r, g, b)$  be a color image, and  $\mathbf{f} \in (E, T^{RGB})$ ,  $\mathbf{f}^c = (r^c, g^c, b^c)$ . The transformation from RGB to HSV color space is given as follows:

$$v = P_1(r, g, b) = \frac{\max \{r, g, b\}}{255}, \quad (8)$$

$$s = P_2(r, g, b) = 1 - \frac{\min \{r, g, b\}}{\max \{r, g, b\}}, \quad (9)$$

$$h = P_3(r, g, b) = \begin{cases} \arccos \left\{ \frac{(r-g)+(r-b)}{2\sqrt{(r-g)^2+(r-b)^2+(g-b)^2}} \right\} & b \leq g \\ 2\pi - \arccos \left\{ \frac{(r-g)+(r-b)}{2\sqrt{(r-g)^2+(r-b)^2+(g-b)^2}} \right\} & b > g \end{cases}, \quad (10)$$

where  $P_1$ ,  $P_2$ , and  $P_3$  are functions of the three variants  $r$ ,  $g$ , and  $b$ , respectively.  $v^c = P'_1(r^c, g^c, b^c) = P'_1(t_{\max} - r, t_{\max} - g, t_{\max} - b)$ ,  $s^c = P'_2(r^c, g^c, b^c) = P'_2(t_{\max} - r, t_{\max} - g, t_{\max} - b)$ , and  $h^c = P'_3(r^c, g^c, b^c) = P'_3(t_{\max} - r, t_{\max} - g, t_{\max} - b)$ .  $P'_1$ ,  $P'_2$  and  $P'_3$  are also functions of the three variants  $r$ ,  $g$ , and  $b$ , respectively. Then,

$$\begin{aligned} &x_1(h_1, s_1, v_1) \leq_{Louverdis} x_2(h_2, s_2, v_2) \\ &\Leftrightarrow x_1(P_1(r_1, g_1, b_1), P_2(r_1, g_1, b_1), P_3(r_1, g_1, b_1)) \leq_{Louverdis} x_2(P_1(r_2, g_2, b_2), P_2(r_2, g_2, b_2), P_3(r_2, g_2, b_2)) \\ &\Leftrightarrow x_1(r_1, g_1, b_1) \leq_{Louverdis} x_2(r_2, g_2, b_2) \\ &\Leftrightarrow \begin{cases} P_1(r_1, g_1, b_1) < P_1(r_2, g_2, b_2) \text{ or} \\ P_1(r_1, g_1, b_1) = P_1(r_2, g_2, b_2) \text{ and } P_2(r_1, g_1, b_1) > P_2(r_2, g_2, b_2) \text{ or} \\ P_1(r_1, g_1, b_1) = P_1(r_2, g_2, b_2) \text{ and } P_2(r_1, g_1, b_1) = P_2(r_2, g_2, b_2) \text{ and } P_3(r_1, g_1, b_1) \leq P_3(r_2, g_2, b_2) \end{cases} \end{aligned}$$

Similarly,

$$\begin{aligned} &x_2^c(h_2, s_2, v_2) \leq_{Louverdis} x_1^c(h_1, s_1, v_1) \\ &\Leftrightarrow \begin{cases} P_1(r_2^c, g_2^c, b_2^c) < P_1(r_1^c, g_1^c, b_1^c) \text{ or} \\ P_1(r_2^c, g_2^c, b_2^c) = P_1(r_1^c, g_1^c, b_1^c) \text{ and } P_2(r_2^c, g_2^c, b_2^c) > P_2(r_1^c, g_1^c, b_1^c) \text{ or} \\ P_1(r_2^c, g_2^c, b_2^c) = P_1(r_1^c, g_1^c, b_1^c) \text{ and } P_2(r_2^c, g_2^c, b_2^c) = P_2(r_1^c, g_1^c, b_1^c) \text{ and } P_3(r_2^c, g_2^c, b_2^c) \leq P_3(r_1^c, g_1^c, b_1^c) \end{cases} \end{aligned}$$

As a result, we obtain  $P_1(r_1, g_1, b_1) \leq P_1(r_2, g_2, b_2) \Leftrightarrow P_1(r_1^c, g_1^c, b_1^c) \geq P_1(r_2^c, g_2^c, b_2^c)$ , but are unable to obtain  $P_2(r_1, g_1, b_1) \leq P_2(r_2, g_2, b_2) \Leftrightarrow P_2(r_1^c, g_1^c, b_1^c) \geq P_2(r_2^c, g_2^c, b_2^c)$  and  $P_3(r_1, g_1, b_1) \leq P_3(r_2, g_2, b_2) \Leftrightarrow P_3(r_1^c, g_1^c, b_1^c) \geq P_3(r_2^c, g_2^c, b_2^c)$  because they are uncertain. Therefore,  $x_1(h_1, s_1, v_1) \leq_{Louverdis} x_2(h_2, s_2, v_2) \Leftrightarrow x_2^c(h_2, s_2, v_2) \leq_{Louverdis} x_1^c(h_1, s_1, v_1)$  is also uncertain, and  $\vee_{\substack{\mathbf{y} \\ \mathbf{y} \in b}} \{ t_{\max} - \mathbf{f}(\mathbf{x} + \mathbf{y}) \} \neq t_{\max} - \wedge_{\substack{\mathbf{y} \\ \mathbf{y} \in b}} \{ \mathbf{f}(\mathbf{x} + \mathbf{y}) \}$ .

Furthermore,

$$\begin{aligned} (\vec{\delta}_{\text{Louverdis}})_b(\mathbf{f}^c) &= \vee_{\substack{\mathbf{y} \in b \\ \mathbf{y} \in \mathbf{f}}} \{\mathbf{f}^c(\mathbf{x} + \mathbf{y})\} \\ &= \vee_{\substack{\mathbf{y} \in b \\ \mathbf{y} \in \mathbf{f}}} \{t_{\max} - \mathbf{f}(\mathbf{x} + \mathbf{y})\} \\ &\neq t_{\max} - \wedge_{\substack{\mathbf{y} \in b \\ \mathbf{y} \in \mathbf{f}}} \{\mathbf{f}(\mathbf{x} + \mathbf{y})\} \\ &= t_{\max} - (\vec{\varepsilon}_{\text{Louverdis}})_b(\mathbf{f}) \\ &= [(\vec{\varepsilon}_{\text{Louverdis}})_b(\mathbf{f})]^c \end{aligned}$$

Therefore, the MMF proposed by Louverdis et al. does not satisfy duality.

The vector ordering depends on  $P_1$ ,  $P_2$ , and  $P_3$ .  $P_i(r_1, g_1, b_1) \leq P_i(r_2, g_2, b_2) \Leftrightarrow P_i(r_1^c, g_1^c, b_1^c) \leq P_i(r_2^c, g_2^c, b_2^c)$ ,  $1 \leq i \leq 3$ , is only correct for linear transformations of RGB color space, i.e.,  $r_1 \leq r_2 \Leftrightarrow r_1^c \leq r_2^c$  because  $r_1 \leq r_2 \Leftrightarrow r_1 - t_{\max} \leq r_2 - t_{\max} \Leftrightarrow t_{\max} - r_1 \leq t_{\max} - r_2 \Leftrightarrow r_1^c \leq r_2^c$ . Similarly,  $g_1 \leq g_2 \Leftrightarrow g_1^c \leq g_2^c$  and  $b_1 \leq b_2 \Leftrightarrow b_1^c \leq b_2^c$  are also obtained. From the analysis made above,  $x_1 \leq_{\text{Louverdis}} x_2 \Leftrightarrow x_1^c \leq_{\text{Louverdis}} x_2^c$  is also not necessarily true. Similarly, we can prove that multivariate morphological frameworks based on vector orderings, such as  $\leq_{\text{Angulo07}}$ ,  $\leq_{\text{Angulo10}}$ ,  $\leq_{\text{Lei13}}$ , and  $\leq_{\text{Lei14}}$ , do not satisfy duality.

**Example 2.** De Witte et al. [16] proposed color morphological operators in RGB color space. In this approach, the vector ordering  $\leq_{\text{DeWitte}}$  of two pixels  $x_1(r_1, g_1, b_1)$  and  $x_2(r_2, g_2, b_2)$  is defined as follows:

$$x_1(r_1, g_1, b_1) \leq_{\text{DeWitte}} x_2(r_2, g_2, b_2) \Leftrightarrow \begin{cases} d(x_1, Bl) < d(x_2, Bl) \text{ or} \\ d(x_1, Bl) = d(x_2, Bl) \text{ and } d(x_1, Wh) \geq d(x_2, Wh) \end{cases}.$$

However, vector ordering  $\geq_{\text{DeWitte}}$  is defined as

$$x_1(r_1, g_1, b_1) \geq_{\text{DeWitte}} x_2(r_2, g_2, b_2) \Leftrightarrow \begin{cases} d(x_1, Wh) < d(x_2, Wh) \text{ or} \\ d(x_1, Wh) = d(x_2, Wh) \text{ and } d(x_1, Bl) \geq d(x_2, Bl) \end{cases},$$

where  $d$  denotes the Euclidean distance, and

$$d(x, Bl) = \sqrt{(r_x - 0)^2 + (g_x - 0)^2 + (b_x - 0)^2}, \quad (11)$$

$$d(x, Wh) = \sqrt{(255 - r_x)^2 + (255 - g_x)^2 + (255 - b_x)^2}. \quad (12)$$

In the following, we use  $t_{\min}$ ,  $t_{\max}$  to represent 0 and 255, respectively.

De Witte et al. also proposed the definitions of color erosion and dilation, denoted by  $\vec{\varepsilon}_{\text{DeWitte}}$  and  $\vec{\delta}_{\text{DeWitte}}$ , respectively, in terms of the vector ordering  $(\leq_{\text{DeWitte}}, \geq_{\text{DeWitte}})$ . Unfortunately,  $\vec{\varepsilon}_{\text{DeWitte}}$  and  $\vec{\delta}_{\text{DeWitte}}$  do not satisfy the requirements of translation-invariance, and increasingness.

**Proof.** Let us study the duality of the morphological framework proposed by De Witte et al. Analogous to Eqs. (7)–(9),  $d(x, Bl) = P_1(r_x, g_x, b_x)$  and  $d(x, Wh) = P_2(r_x, g_x, b_x)$  are obtained, where  $P_1$  and  $P_2$  are functions of the three variants  $r$ ,  $g$ , and  $b$ . Then,

$$\begin{aligned} x_1(r_1, g_1, b_1) \leq_{\text{DeWitte}} x_2(r_2, g_2, b_2) \\ \Leftrightarrow \begin{cases} P_1(r_1, g_1, b_1) < P_1(r_2, g_2, b_2) \text{ or} \\ P_1(r_1, g_1, b_1) = P_1(r_2, g_2, b_2) \text{ and } P_2(r_1, g_1, b_1) \geq P_2(r_2, g_2, b_2) \end{cases}, \end{aligned}$$

$$\begin{aligned} x_1(r_1, g_1, b_1) \geq_{\text{DeWitte}} x_2(r_2, g_2, b_2) \\ \Leftrightarrow \begin{cases} P_2(r_1, g_1, b_1) < P_2(r_2, g_2, b_2) \text{ or} \\ P_2(r_1, g_1, b_1) = P_2(r_2, g_2, b_2) \text{ and } P_1(r_1, g_1, b_1) \geq P_1(r_2, g_2, b_2) \end{cases}, \end{aligned}$$

$$\begin{aligned} x_1^c(r_1, g_1, b_1) \leq_{\text{DeWitte}} x_2^c(r_2, g_2, b_2) \\ \Leftrightarrow \begin{cases} P_2(r_1^c, g_1^c, b_1^c) < P_2(r_2^c, g_2^c, b_2^c) \text{ or} \\ P_2(r_1^c, g_1^c, b_1^c) = P_2(r_2^c, g_2^c, b_2^c) \text{ and } P_1(r_1^c, g_1^c, b_1^c) \geq P_1(r_2^c, g_2^c, b_2^c) \end{cases}, \end{aligned}$$

$$\begin{aligned} d(x_1^c, Bl) &= \sqrt{(t_{\max} - r_1)^2 + (t_{\max} - g_1)^2 + (t_{\max} - b_1)^2} \\ &= d(x_1, Wh) \end{aligned}$$

and

$$\begin{aligned} d(x_1^c, Wh) &= \sqrt{(t_{\max} - (t_{\max} - r_1))^2 + (t_{\max} - (t_{\max} - g_1))^2 + (t_{\max} - (t_{\max} - b_1))^2} \\ &= \sqrt{(r_1)^2 + (g_1)^2 + (b_1)^2} = d(x_1, Bl) \end{aligned}$$

We then get

$$P_2(r_1^c, g_1^c, b_1^c) = \sqrt{(t_{\max} - r_1^c)^2 + (t_{\max} - g_1^c)^2 + (t_{\max} - b_1^c)^2}$$

because  $r_1^c = t_{\max} - r_1$ ,  $g_1^c = t_{\max} - g_1$ ,  $b_1^c = t_{\max} - b_1$ ,

$$\begin{aligned} P_2(r_1^c, g_1^c, b_1^c) &= \sqrt{(r_1)^2 + (g_1)^2 + (b_1)^2} \text{ and} \\ &= P_1(r_1, g_1, b_1) \end{aligned}$$

$$\begin{aligned} &\left\{ \begin{array}{l} P_2(r_1^c, g_1^c, b_1^c) < P_2(r_2^c, g_2^c, b_2^c) \text{ or} \\ P_2(r_1^c, g_1^c, b_1^c) = P_2(r_2^c, g_2^c, b_2^c) \text{ and } P_1(r_1^c, g_1^c, b_1^c) \geq P_1(r_2^c, g_2^c, b_2^c) \end{array} \right., \\ &\Leftrightarrow \left\{ \begin{array}{l} P_1(r_1, g_1, b_1) < P_1(r_2, g_2, b_2) \text{ or} \\ P_1(r_1, g_1, b_1) = P_1(r_2, g_2, b_2) \text{ and } P_2(r_1, g_1, b_1) \geq P_2(r_2, g_2, b_2) \end{array} \right. \end{aligned}$$

i.e.,

$$x_1^c(r_1, g_1, b_1)_{De\ Witte} \geq x_2^c(r_2, g_2, b_2) \Leftrightarrow x_1(r_1, g_1, b_1)_{De\ Witte} \geq x_2(r_2, g_2, b_2).$$

Then,

$$\begin{aligned} (\vec{\delta}_{De\ Witte})_b(\mathbf{f}) &= \vee_{\mathbf{y} \in b} \{\mathbf{f}(\mathbf{x} + \mathbf{y})\} \\ &= \vee_{\mathbf{y} \in b} \{t_{\max} - \mathbf{f}(\mathbf{x} + \mathbf{y})\} \\ &= t_{\max} - \wedge_{\mathbf{y} \in b} \{\mathbf{f}(\mathbf{x} + \mathbf{y})\} \\ &= t_{\max} - (\vec{\epsilon}_{De\ Witte})_b(\mathbf{f}) \\ &= [(\vec{\epsilon}_{De\ Witte})_b(\mathbf{f})]^c \end{aligned}$$

Therefore,

$$\begin{aligned} &x_1^c(r_1^c, g_1^c, b_1^c)_{De\ Witte} \geq x_2^c(r_2^c, g_2^c, b_2^c) \\ &\Leftrightarrow \left\{ \begin{array}{l} d(x_1^c, Bl) < d(x_2^c, Bl) \text{ or} \\ d(x_1^c, Bl) = d(x_2^c, Bl) \text{ and } d(x_1^c, Wh) \geq d(x_2^c, Wh) \end{array} \right. \\ &\Leftrightarrow \left\{ \begin{array}{l} d(x_1, Wh) < d(x_2, Wh) \text{ or} \\ d(x_1, Wh) = d(x_2, Wh) \text{ and } d(x_1, Bl) \geq d(x_2, Bl) \end{array} \right. \\ &\Leftrightarrow x_1(r_1, g_1, b_1)_{De\ Witte} \geq x_2(r_2, g_2, b_2) \end{aligned}$$

Accordingly, the MMOs proposed by De Witte et al. satisfy duality. However, these MMOs are called pseudo morphological operators since  $\leq_{De\ Witte}$  and  $\geq_{De\ Witte}$  are two different vector orderings and are defined in two different lattices.

To further illustrate Examples 1, 2 and Fig. 6 shows the ordering results of color pixels.

In Fig. 6,  $(\vec{\epsilon}_{De\ Witte})_b(\mathbf{f}) = ((\vec{\delta}_{De\ Witte})_b(\mathbf{f}))^c = (55, 55, 75)$  and  $(\vec{\delta}_{De\ Witte})_b(\mathbf{f}) = ((\vec{\epsilon}_{De\ Witte})_b(\mathbf{f}))^c = (200, 200, 180)$ , and it is clear that  $(\vec{\epsilon}_{De\ Witte}, \vec{\delta}_{De\ Witte})$  is a pair of dual MMOs. However,  $(\vec{\epsilon}_{Louverdis})_b(\mathbf{f}) = (55, 55, 75)$ ,  $(\vec{\delta}_{Louverdis})_b(\mathbf{f}) = (255, 255, 50)$ ,  $((\vec{\delta}_{Louverdis})_b(\mathbf{f}))^c = (0, 0, 205)$ , and  $((\vec{\epsilon}_{Louverdis})_b(\mathbf{f}))^c = (200, 200, 180)$ , thus,  $(\vec{\epsilon}_{Louverdis})_b(\mathbf{f}) \neq ((\vec{\delta}_{Louverdis})_b(\mathbf{f}))^c$  and  $(\vec{\delta}_{Louverdis})_b(\mathbf{f}) \neq ((\vec{\epsilon}_{Louverdis})_b(\mathbf{f}))^c$ . It is clear that  $(\vec{\epsilon}_{Louverdis}, \vec{\delta}_{Louverdis})$  is not a pair of dual MMOs.

Based on the results of these examples, we summarize the factors that affect the property of duality of MMOs. In Example 1, the authors constructed MMOs in HSV color space. These MMOs are not dual since the transformation from RGB to HSV is nonlinear. In Example 2, the authors proposed vector ordering based on the Euclidean distance in the RGB color space. Although these MMOs are dual, they are defined in two different lattices because the corresponding vector ordering relies on two reference colors. Therefore, an accurate vector ordering should satisfy two conditions:

- (1) The vector ordering must be defined in a complete lattice.
- (2) There is a linear transformation system from RGB to other spaces in which multivariate dual morphological operators are defined.

#### 4. Multivariate dual morphological systems

The transformation from RGB to YUV color space is linear, i.e.,

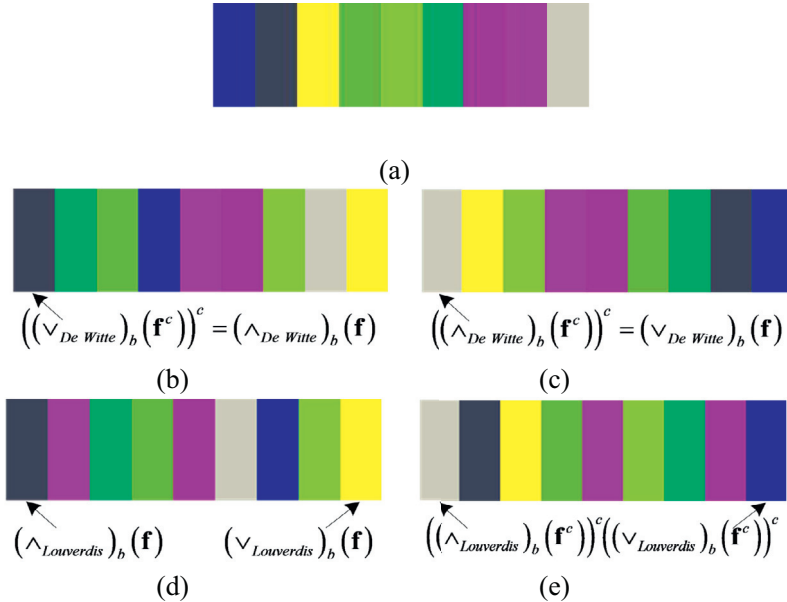


**Fig. 6.** Vector ordering results using  $\leq_{Louverdis}$ ,  $\leq_{DeWitte} \geq$ , and  $\leq_{DeWitte}$ , respectively. (a) Original color pixel set  $\mathbf{f}$ . (b) Ordering result of  $\mathbf{f}$  using  $\leq_{DeWitte}$ . (c) Ordering result of  $\mathbf{f}^c$  using  $\leq_{DeWitte} \geq$ . (d) Ordering result of  $\mathbf{f}$  using  $\leq_{Louverdis}$ . (e) Ordering result of  $\mathbf{f}^c$  using  $\leq_{Louverdis}$ .

$$\bar{v}'(y, u, v) = T[\bar{v}(r, g, b)] \Leftrightarrow \begin{cases} y = T_y(r, g, b) \\ u = T_u(r, g, b), \\ v = T_v(r, g, b) \end{cases} \quad (13)$$

where  $T\{T_y, T_u, T_v\}$  is a linear transformation system from RGB to YUV. Based on the two conditions mentioned above, we first propose a MMF based on a color space transformation as follows:

$$\bar{v}'_1(y_1, u_1, v_1) \leq_{YUV} \bar{v}'_2(y_2, u_2, v_2) \Leftrightarrow \begin{cases} y_1 < y_2 \text{ or} \\ y_1 = y_2 \text{ and } u_1 < u_2 \text{ or} \\ y_1 = y_2 \text{ and } u_1 = u_2 \text{ and } v_1 \leq v_2 \end{cases}. \quad (14)$$

First, YUV is a linear transformation of RGB color space. Second, relation 14 is a vector ordering in a complete lattice  $(\mathcal{T}, \leq_{YUV})$ . Finally, Y denotes the brightness in YUV color space, which is of a higher rank than color components U and V in terms of visual perception. Therefore,  $(\mathcal{T}, \leq_{YUV})$  satisfies the two conditions of an accurate vector ordering, and is able to be used to define MMOs with duality.

Similarly, YIQ and YCbCr are the linear transformations of RGB color space, and are also able to be used to define MMOs with duality in terms of  $(\mathcal{T}, \leq_{YIQ})$  and  $(\mathcal{T}, \leq_{YCbCr})$ . However, how can we define the pairwise ranks between color components such as (U, V), (I, Q), and (Cb, Cr)? In fact, there is no specific ordering between U and V (I and Q, Cb and Cr). Thus, to propose a better vector ordering, we introduce PCA into our system because a decided ordering exists among different PCA components, i.e., the first component is more important than the second, the second is more important than the third, and so on.

$$\bar{v}'_1(f_1^p, s_1^p, t_1^p) \leq_{PCA} \bar{v}'_2(f_2^p, s_2^p, t_2^p) \Leftrightarrow \begin{cases} f_1^p < f_2^p \text{ or} \\ f_1^p = f_2^p \text{ and } s_1^p < s_2^p \text{ or} \\ f_1^p = f_2^p \text{ and } s_1^p = s_2^p \text{ and } t_1^p \leq t_2^p \end{cases}, \quad (15)$$

where  $f^p$ ,  $s^p$ , and  $t^p$  denote the first, second, and third principal components respectively. Since PCA is a popular dimensional reduction algorithm, it is easy to extend relation (15) to high-dimension data processing. (The signs of the projection vectors from PCA are arbitrary. Here, we only use PCA to reduce the dimensions. Each dimension of the reduced subspace has the same direction, and thus the signs do not influence the result.) Depending on relation (15), we define a linear transformation system based on PCA, where  $\bar{v}(d_1, d_2, \dots, d_n)$  denotes the original high-dimension data, and  $\bar{v}'(D_1, D_2, \dots, D_n)$  denotes the transformed high-dimension data using a linear system  $T\{T_1, T_2, \dots, T_n\}$ ,  $n \in R$ , i.e.,

$$\bar{v}'(D_1, D_2, \dots, D_n) = T[\bar{v}(d_1, d_2, \dots, d_n)] \Leftrightarrow \begin{cases} D_1 = T_1(d_1, d_2, \dots, d_n) \\ D_2 = T_2(d_1, d_2, \dots, d_n) \\ \vdots \\ D_n = T_n(d_1, d_2, \dots, d_n) \end{cases}, \quad (16)$$

$$\vec{v}_1^r \leq_{PCA} \vec{v}_2^r \Leftrightarrow \begin{cases} T_1[\vec{v}_1] < T_1[\vec{v}_2] \text{ or} \\ T_1[\vec{v}_1] = T_1[\vec{v}_2] \text{ and } T_2[\vec{v}_1] < T_2[\vec{v}_2] \text{ or} \\ \vdots \\ T_1[\vec{v}_1] = T_1[\vec{v}_2] \text{ and } T_2[\vec{v}_1] = T_2[\vec{v}_2] \cdots \text{ and } T_n[\vec{v}_1] \leq T_n[\vec{v}_2] \end{cases}. \quad (17)$$

However, the lexicographic ordering  $\leq_{PCA}$  is so huge that when the value of  $n$  is large, it leads to a high computational cost. Fortunately, we can reduce the value of  $n$  by selecting the first  $m$  principal components that include the main information of the data.  $m \ll n$  when the value of  $n$  is extremely large, for example,  $n=225$  for hyperspectral remote sensing images.

Based on the above analysis, the proposed vector ordering not only protects duality, but is also easily carried out. Finally, based on the different color spaces and PCA, we propose a unified representation form of the vector ordering ( $\leq_{LT}$ ) that includes  $\leq_{YUV}$ ,  $\leq_{YIQ}$ ,  $\leq_{YCrcb}$ , and  $\leq_{PCA}$ , where  $m=3$  for  $\leq_{YUV}$ ,  $\leq_{YIQ}$ , and  $\leq_{YCrcb}$ , and  $3 \leq m \leq n$  for  $\leq_{PCA}$ .

Let  $\mathbf{f}$  denote a color image, and  $(\mathcal{T}; \leq_{LT})$  be a completed lattice ordering.  $\vee_{LT}$  and  $\wedge_{LT}$  denote the supremum and infimum based on  $\leq_{LT}$ , respectively. We define the unified multivariate morphological erosion and dilation as follows:

$$(\vec{\epsilon}_{LT})_b(\mathbf{f}) = \wedge_{LT} \underset{t \in b}{\vee} (\mathbf{f}_{-t}), \quad (20)$$

$$(\vec{\delta}_{LT})_b(\mathbf{f}) = \vee_{LT} \underset{t \in b}{\wedge} (\mathbf{f}_{-t}), \quad (21)$$

where  $(\vec{\epsilon}_{LT}, \vec{\delta}_{LT})$  is an adjunction. We analyze the properties of  $\vec{\epsilon}_{LT}$  and  $\vec{\delta}_{LT}$  in the following.

**Definition 6.** The transformation  $\psi$  is invariant to translations if it commutes with image translations, i.e.,

$$\psi \text{ is invariant to translations} \Leftrightarrow \forall f, \forall b, \psi(f_k) = [\psi(f)]_k.$$

**Proposition 1.** If  $\vec{\epsilon}_{LT}$  and  $\vec{\delta}_{LT}$  are multivariate erosion and dilation based on vector ordering  $\leq_T$ , then

$$\vec{\epsilon}_{LT} \text{ is invariant to translations} \Leftrightarrow [(\vec{\epsilon}_{LT})_b(\mathbf{f})]_k + \mathbf{r} = (\vec{\epsilon}_{LT})_b(\mathbf{f}_k + \mathbf{r}), \text{ and}$$

$$\vec{\delta}_{LT} \text{ is invariant to translations} \Leftrightarrow [(\vec{\delta}_{LT})_b(\mathbf{f})]_k + \mathbf{r} = (\vec{\delta}_{LT})_b(\mathbf{f}_k + \mathbf{r}).$$

### Proof.

$$\begin{aligned} (\vec{\epsilon}_{LT})_b(\mathbf{f}_k + \mathbf{r})(\mathbf{x}) &= \inf_{\mathbf{y} \in \overset{\vee}{b}} \{\mathbf{f}_k(\mathbf{x} + \mathbf{y}) + \mathbf{r}\} \\ &= \wedge_T \underset{\mathbf{y} \in \overset{\vee}{b}}{\{\mathbf{f}(\mathbf{x} + \mathbf{y})\}}_k + \mathbf{r} \\ &= \left( \wedge_T \underset{\mathbf{y} \in \overset{\vee}{b}}{\{\mathbf{f}(\mathbf{x} + \mathbf{y})\}} \right)_k + \mathbf{r} \\ &= [(\vec{\epsilon}_{LT})_b(\mathbf{f})(\mathbf{x})]_k + \mathbf{r} \end{aligned}$$

Similarly,  $(\vec{\delta}_{LT})_b(\mathbf{f}_k + \mathbf{r})(\mathbf{x}) = [(\vec{\delta}_{LT})_b(\mathbf{f})(\mathbf{x})]_k + \mathbf{r}$ .

**Definition 7.** The transformation  $\psi$  is extensive if, for a multi-channel image  $\mathbf{f}$ , the transformed image is greater than or equal to the original image, i.e., if  $\psi$  is greater than or equal to the identity transformation  $id$ , then

$$\psi \text{ is extensive} \Leftrightarrow id \leq_{LT} \psi.$$

**Definition 8.** The transformation  $\psi$  is anti-extensive if, for a multi-channel image  $\mathbf{f}$ , the transformed image is less than or equal to the original image, i.e., if  $\psi$  is less than or equal to the identity transformation  $id$ , then

$$\psi \text{ is anti-extensive} \Leftrightarrow \psi \leq_{LT} id.$$

**Proposition 2.** If  $\vec{\epsilon}_{LT}$  and  $\vec{\delta}_{LT}$  are multivariate erosion and dilation based on vector ordering  $\leq_{LT}$ , then

$$\vec{\delta}_{LT} \text{ is extensive} \Leftrightarrow id \leq_{LT} \vec{\delta}_{LT}, \text{ and}$$

$$\vec{\epsilon}_{LT} \text{ is anti-extensive} \Leftrightarrow \vec{\epsilon}_{LT} \leq_{LT} id.$$

**Proof.**

$$\begin{aligned} (\vec{\epsilon}_{LT})_b(\mathbf{f})(\mathbf{x}) &= \inf_{\substack{\mathbf{y} \\ \mathbf{y} \in b}} \{\mathbf{f}(\mathbf{x} + \mathbf{y})\} \\ &= \wedge_{\substack{\mathbf{y} \\ \mathbf{y} \in b}} \{\mathbf{f}(\mathbf{x} + \mathbf{y})\} \end{aligned}$$

$\forall \mathbf{x}_i \in \mathbf{f}, \exists \vec{\epsilon}(\mathbf{f})(\mathbf{x}_i) \leq_{LT} \mathbf{x}_i$ , i.e.,  $\vec{\epsilon}_{LT} \leq_{LT} id$ . Similarly,  $id \leq_T \vec{\delta}_{LT}$ .

**Definition 9.** The transformation  $\psi$  is increasing if it preserves the ordering relations between images, i.e.,

$$\psi \text{ is increasing} \Leftrightarrow \forall \mathbf{f}, \mathbf{g}, \mathbf{f} \leq_{LT} \mathbf{g} \Rightarrow \psi(\mathbf{f}) \leq_{LT} \psi(\mathbf{g}).$$

**Proposition 3.** If  $\vec{\epsilon}_{LT}$  and  $\vec{\delta}_{LT}$  are multivariate erosion and dilation based on vector ordering  $\leq_{LT}$ , then

$$\vec{\delta}_{LT} \text{ is increasing} \Leftrightarrow \mathbf{f} \leq_{LT} \mathbf{g} \Rightarrow \vec{\delta}_{LT}(\mathbf{f}) \leq_{LT} \vec{\delta}_{LT}(\mathbf{g}), \text{ and}$$

$$\vec{\epsilon}_{LT} \text{ is increasing} \Leftrightarrow \mathbf{f} \leq_{LT} \mathbf{g} \Rightarrow \vec{\epsilon}_{LT}(\mathbf{f}) \leq_{LT} \vec{\epsilon}_{LT}(\mathbf{g}).$$

**Proof.** If  $\forall \mathbf{x}_i \in \mathbf{f}, \forall \mathbf{z}_i \in \mathbf{g}$ , then  $\mathbf{x}_i \leq_{LT} \mathbf{z}_i$  for  $\mathbf{f} \leq_{LT} \mathbf{g}$ .  $\mathbf{x}_i + \mathbf{y} \leq_{LT} \mathbf{z}_i + \mathbf{y}$ , so  $\wedge_{\substack{\mathbf{y} \\ \mathbf{y} \in b}} (\mathbf{x}_i + \mathbf{y}) \leq_{LT} \wedge_{\substack{\mathbf{y} \\ \mathbf{y} \in b}} (\mathbf{z}_i + \mathbf{y})$ , i.e.  $\vec{\epsilon}_b(\mathbf{f}) \leq_{LT} \vec{\epsilon}_b(\mathbf{g})$ . Similarly,  $\mathbf{f} \leq_{LT} \mathbf{g} \Rightarrow \vec{\delta}(\mathbf{f}) \leq_{LT} \vec{\delta}(\mathbf{g})$ .

**Proposition 4.** If  $\vec{\epsilon}_{LT}$  and  $\vec{\delta}_{LT}$  are multivariate erosion and dilation based on vector ordering  $\leq_{LT}$ , then  $\vec{\epsilon}_{LT}$  and  $\vec{\delta}_{LT}$  are dual forms with respect to complementation  $C \Leftrightarrow \vec{\epsilon}_{LT} = C \vec{\delta}_{LT} C$ .

**Proof.**

$$\begin{aligned} (\vec{\delta}_{LT})_b(\mathbf{f}^c) &= \sup_{\substack{\mathbf{y} \\ \mathbf{y} \in b}} \{\mathbf{f}^c(\mathbf{x} + \mathbf{y})\} \\ &= \vee_{\substack{\mathbf{y} \\ \mathbf{y} \in b}} \{\mathbf{f}^c(\mathbf{x} + \mathbf{y})\} \\ &= \vee_{\substack{\mathbf{y} \\ \mathbf{y} \in b}} \{t_{\max} - \mathbf{f}(\mathbf{x} + \mathbf{y})\} \\ &= t_{\max} - \wedge_{\substack{\mathbf{y} \\ \mathbf{y} \in b}} \{\mathbf{f}(\mathbf{x} + \mathbf{y})\} \\ &= t_{\max} - \vec{\epsilon}_b(\mathbf{f}^c) \\ &= [(\vec{\epsilon}_{LT})_b(\mathbf{f}^c)]^c \end{aligned}$$

The proposed vector ordering  $\leq_{LT}$  is a framework in which classical grayscale morphological algorithms can be easily extended to multi-channel images.

## 5. Experimental results and analysis

It is well-known that MMOs are widely used in image filtering, edge detection, image enhancement, and image segmentation. However, it is difficult to evaluate the performance of morphological operators due to different user requirements. To demonstrate that the proposed multivariate morphological framework is useful for color image processing, erosion and dilation are applied to color images to show that the proposed MMOs have the property of duality. We then conduct an image filtering experiment to show that the proposed multivariate morphological opening and closing achieve similar filtering effects and preserve some important properties of traditional morphological filters. Finally, we conduct an image segmentation experiment to show the viability of extending traditional MMOs into the proposed MMF.

### 5.1. Color image erosions and dilations

To show that the proposed MMF maintains the duality, five MMFs (shown in Table 1) and the proposed MMF were applied in color image erosions and dilations with an square structure element of size  $11 \times 11$ . Fig. 7 shows that  $\vec{\epsilon} \neq (\vec{\delta}(\mathbf{f}^c))^c$  for multivariate morphological approaches based on VSH, DLSH, QPEPA, HVSD and FEEA. According to Definition 3,  $(\vec{\epsilon}_{Louverdis}, \vec{\delta}_{Louverdis})$ ,  $(\vec{\epsilon}_{Angulo\,07}, \vec{\delta}_{Angulo\,07})$ ,  $(\vec{\epsilon}_{Angulo\,10}, \vec{\delta}_{Angulo\,10})$ ,  $(\vec{\epsilon}_{Lei\,13}, \vec{\delta}_{Lei\,13})$  and  $(\vec{\epsilon}_{Lei\,14}, \vec{\delta}_{Lei\,14})$  satisfy duality. However, the proposed MMF maintains the duality because  $\vec{\epsilon} = (\vec{\delta}(\mathbf{f}^c))^c$  (we replaced  $[\vec{\epsilon} - (\vec{\delta}(\mathbf{f}^c))^c]$  with  $[\vec{\epsilon} - (\vec{\delta}(\mathbf{f}^c))^c]^c$  to facilitate observation in the far right of Fig. 7).



**Fig. 7.** Images produced by  $\bar{\epsilon}$  and  $(\bar{\delta}(\mathbf{f}^c))^c$  to demonstrate that existing multivariate morphological approaches violate duality while the proposed MMF maintains duality. (a) VSH. (b) DLSH. (c) QPEPA. (d) HVSD. (e) FEEA. (f) Our-YUV. (g) Our-PCA.

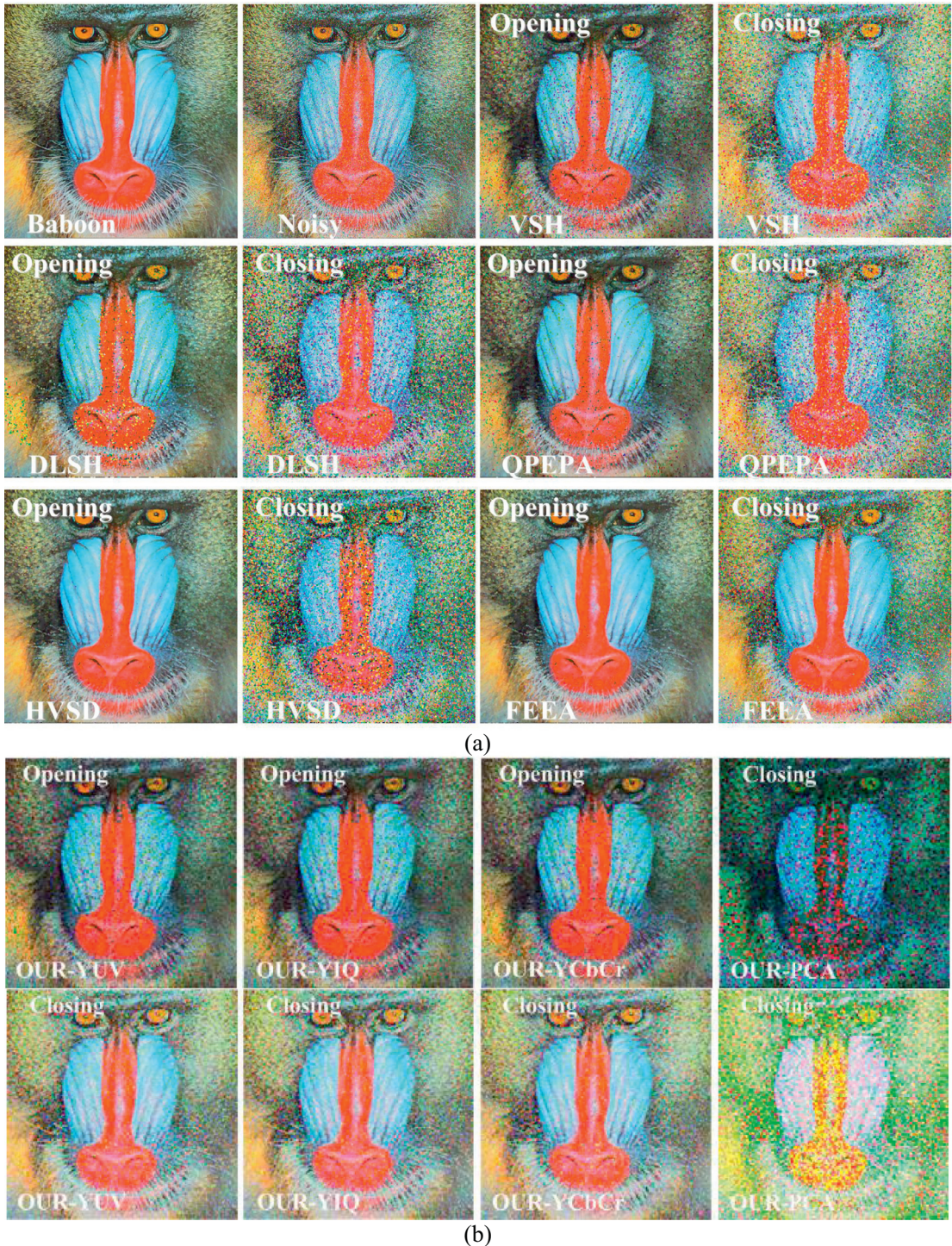


**Fig. 8.** Noise removal using multivariate openings and closings defined in different MMFs. (a) Existing MMFs. (b) Our proposed MMF.

## 5.2. Color image filtering

Classical morphological operators have been widely used in binary and grayscale image processing. The proposed MMF can be used to build any of the advanced operators described in the literature of mathematical morphology. To demonstrate the effectiveness and duality of the proposed MMF, we used the “Baboon” image (image size  $512 \times 512$ ), and the salt & pepper noise model in the following experiments. The density of the impulsive noise was 10%. We adopted morphological

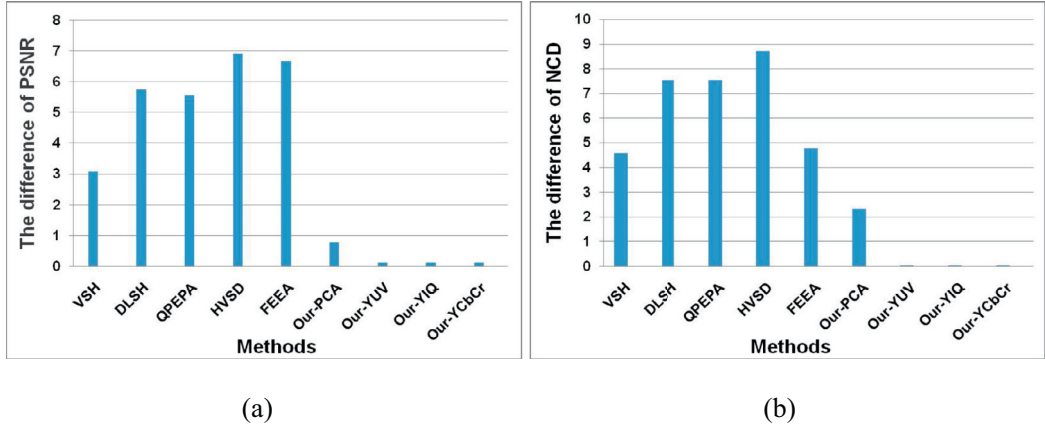


Fig. 9. Differences in performance of multivariate morphological openings and closings. (a) PSNR. (b) NCD.

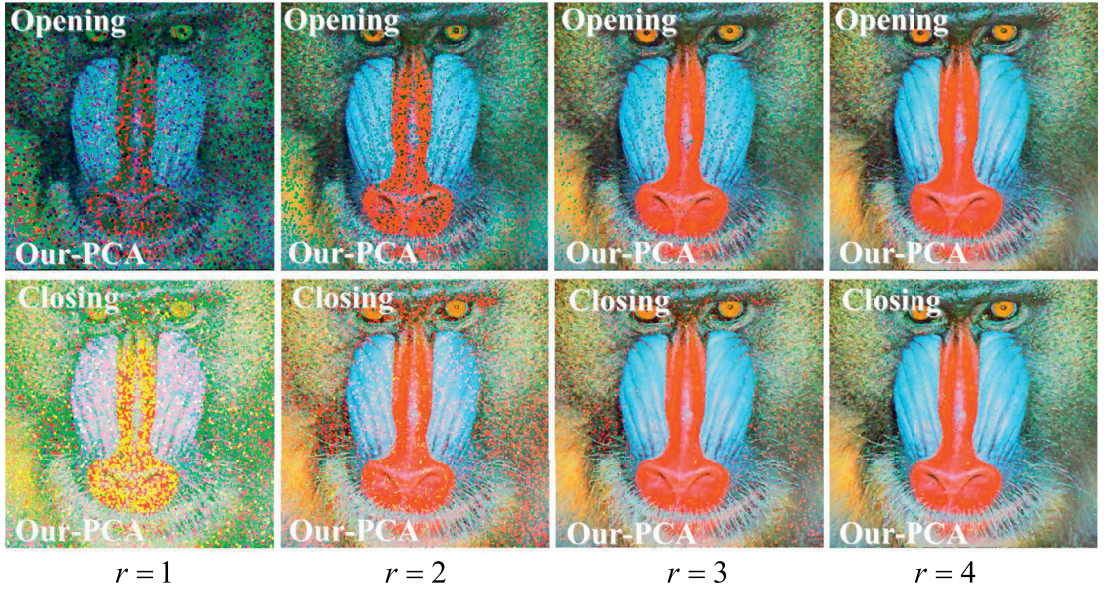


Fig. 10. Noise removal using multivariate soft openings and closings defined in the proposed MMF.

opening and closing filters to remove the noise. Fig. 8(a) and (b) show the filtering results obtained by opening and closing based on the existing MMFs and the proposed MMF, respectively. For the sake of fairness, all filters adopted the same structuring element, a square of size  $3 \times 3$ .

Fig. 8(a) shows that the multivariate morphological opening filters are able to suppress noise while the closing filters fail to suppress noise. These results are caused by the non-duality of existing MMFs. In Fig. 8(b), although the proposed multivariate opening and closing are unable to provide better filtering results, they achieve similar filtering performance because they satisfy duality. Note that the goal of this experiment is not to show that the proposed framework outperforms the other methods for noise removal, but that the proposed MMF satisfies duality.

PSNR and normalized color difference (NCD), two quantitative measures, are commonly used for measuring restoration quality,

$$PSNR(\mathbf{f}, \mathbf{g}) = 10\log_{10} \frac{3 \times M \times N \times 255^2}{\sum_{i=1}^M \sum_{j=1}^N \|\mathbf{f}(i, j) - \mathbf{g}(i, j)\|^2}, \quad (22)$$

$$NCD(\mathbf{f}, \mathbf{g}) = \frac{\sum_{i=1}^M \sum_{j=1}^N \|\mathbf{f}_{L*a*b*}(i, j) - \mathbf{g}_{L*a*b*}(i, j)\|^2}{\sum_{i=1}^M \sum_{j=1}^N \|\mathbf{f}_{L*a*b*}(i, j)\|^2}. \quad (23)$$

where  $\mathbf{f}$  is the original color image and  $\mathbf{g}$  is the filtered image of size  $M \times N$ .

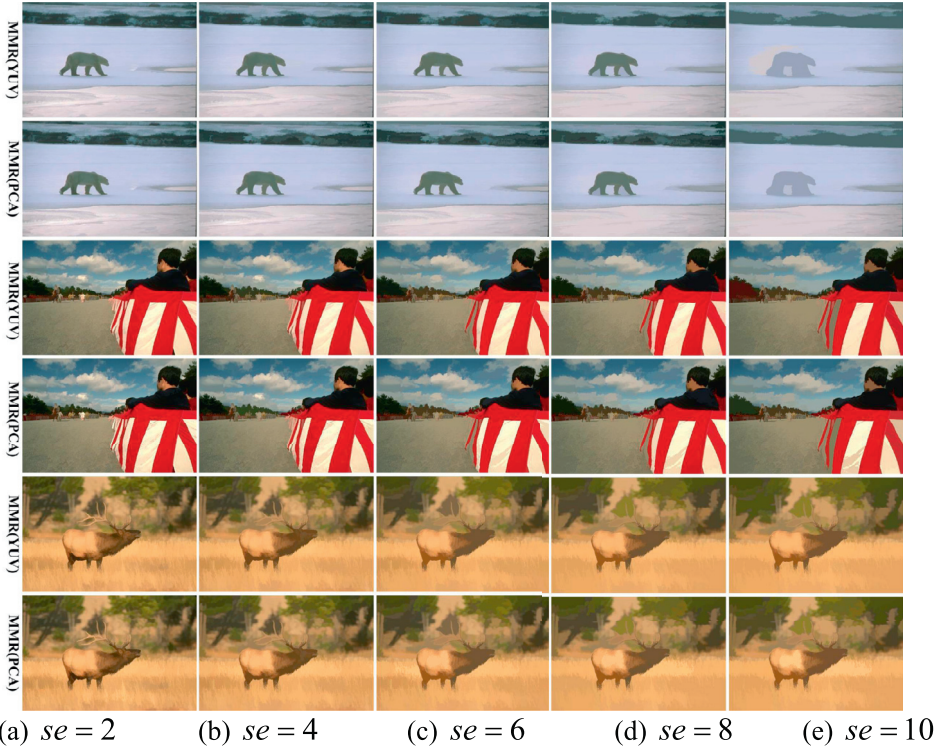


**Fig. 11.** Reconstruction results from the proposed multivariate morphological opening reconstruction.

To further illustrate this result, Figs. 8 and 9 show performance comparisons for multivariate openings and closings. In Fig. 9, it is clear that there are large differences in PSNR and NCD between multivariate openings and closings defined by existing MMFs. In contrast, a small difference between those in the proposed MMF shows that the multivariate opening and closing operators achieve a similar performance. Consequently, the proposed MMF has the same properties as the classical grayscale morphological framework, and these properties can be unified in a morphological framework.

Figs. 8 and 9 shows that the proposed MMF addresses the problem of existing MMOs not satisfying duality. Hence, classical morphological approaches can be directly extended to multi-channel image processing in terms of the proposed MMF.

To easily extend classical morphological algorithms to the proposed MMF, we also propose multivariate soft morphological operators [23,25] in this paper. Depending on the proposed vector ordering  $\leq_{LT}$ , the multivariate soft morphological erosion of  $\mathbf{f}$  by a soft structuring element  $[b, A, r]$  is defined as,

$$\bar{\varepsilon}_{LT}^{soft}(\mathbf{f}, [b, A, r])(\mathbf{x}) = \text{rth smallest of } \{r \diamond \mathbf{f}(\mathbf{a}) : \mathbf{a} \in A_{\mathbf{x}}\} \cup \{\mathbf{f}(\mathbf{b}) : \mathbf{b} \in (b \setminus A_{\mathbf{x}})\}. \quad (24)$$

Similarly, the multivariate soft morphological dilation of  $\mathbf{f}$  by  $[b, A, r]$  is defined as,

$$\bar{\delta}_{LT}^{soft}(\mathbf{f}, [b, A, r])(\mathbf{x}) = \text{rth largest of } \{r \diamond \mathbf{f}(\mathbf{a}) : \mathbf{a} \in A_{\mathbf{x}}\} \cup \{\mathbf{f}(\mathbf{b}) : \mathbf{b} \in (b \setminus A_{\mathbf{x}})\}. \quad (25)$$

where  $\diamond$  represents the repetitive operation of any object.  $r \diamond \mathbf{f}(\mathbf{a})$  denotes the repetition of  $\mathbf{f}(\mathbf{a})$  ( $r$  times), i.e.,  $r \diamond \mathbf{f}(\mathbf{a}) = \underbrace{\{\mathbf{f}(\mathbf{a}), \mathbf{f}(\mathbf{a}), \dots, \mathbf{f}(\mathbf{a})\}}_{r \text{ times}}$ . The structuring element  $b$  is divided into two subsets: the core  $A$  and the soft boundary  $B \setminus A$ , where ‘\’ represents the set difference.

Based on  $\bar{\varepsilon}_{LT}^{soft}$  and  $\bar{\delta}_{LT}^{soft}$ , we apply multivariate soft opening ( $\bar{\delta}_{LT}^{soft}(\bar{\varepsilon}_{LT}^{soft})$ ) and closing operators ( $\bar{\varepsilon}_{LT}^{soft}(\bar{\delta}_{LT}^{soft})$ ) to impulse noise suppression. Fig. 10 shows the filtering results (We employed multivariate soft opening and closing to filter image noise. Let  $r$  ( $1 \leq r \leq 4$ ) be the rank of soft morphological operators. The structuring element was a disk of size  $5 \times 5$ .) Clearly, the proposed multivariate soft morphological operators perform better with increasing  $r$  values.

### 5.3. Color image reconstruction and segmentation

It is well-known that morphological reconstruction is able to remove texture details while protecting object contours in images. Based on the proposed MMF, we extend multivariate morphological reconstruction (MMR) operations to color image processing. The proposed MMR operations were conducted on the BSDS500 dataset. Fig. 11 shows the reconstruction results

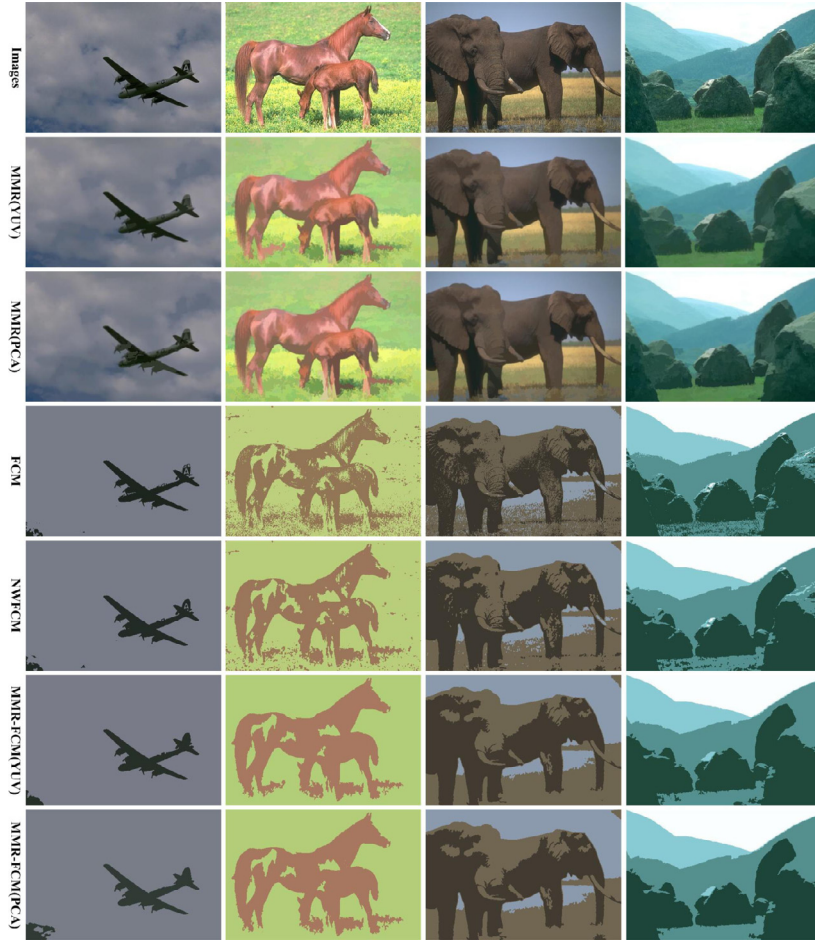


Fig. 12. Segmentation results from different approaches.

**Table 2**  
CPU time consumption of the different segmentation approaches (unit: s).

Image	FCM	NWFCM	MMR-FCM(YUV)	MMR-FCM(PCA)
3096	2.02	8.99	3.13	3.14
113,044	2.07	9.15	3.16	3.15
296,059	2.05	9.09	3.14	3.13
241,004	2.04	9.11	3.13	3.14
Average	2.045	9.085	<b>3.14</b>	<b>3.135</b>

from the proposed MMR with different-sized structuring elements ( $se$  represents the radius of a circular structuring element). As shown in Fig. 11, with the increase of  $se$ , more texture details are removed while object contours are preserved, showing that MMR is useful for image simplification. In addition, MMR is also used to improve the segmentation result. The fuzzy c-means (FCM) [10] algorithm is a popular algorithm for color image segmentation. However, the traditional FCM algorithm provides poor segmentation results since it ignores spatial information. Although some improved algorithms which incorporate local information into the FCM algorithm, can obtain better image segmentation results, a high computational cost limits their applications [17,27]. Because MMR can smooth noise and texture detail, and also preserve accurate boundaries in color images, we apply MMR to FCM to improve segmentation results. Fig. 12 shows the segmentation results generated by FCM and the improved FCM algorithms. (In this paper, we first used MMR to simplify a color image, and then employed FCM to segment the simplified image. These methods are denoted by MMR-FCM (YUV) and MMR-FCM (PCA).)

As shown in Fig. 11, NWFCM [46] provides better segmentation than FCM since the former employs the spatial neighbor information. In comparison to NWFCM, the proposed MMR-FCM (YUV) and MMR-FCM (PCA) provide better segmentation results because MMR is utilized to improve FCM. Moreover, the proposed MMR-FCM has lower computational complexity than NWFCM. Table 2 shows the CPU time consumption of the different approaches, and that the proposed MMR-FCM requires less CPU time than NWFCM.

## 6. Conclusions

In this paper, we demonstrated that existing MMFs do not satisfy duality. To address this problem, we proposed a conditionally invariant MMF based on a linear transformation system, such as YUV, YIQ, and YCbCr color space, or PCA. The proposed MMF was able to be directly applied to color image processing, and provided some useful results due to the duality principle. We also constructed MMOs and applied them to color image processing including image filtering, reconstruction and segmentation. Our experimental results demonstrated the superiority of the proposed MMF, indicating promising prospects for future applications.

## Acknowledgment

This work was supported by the National Natural Science Foundation of China (Grant Nos. 61461025, 61672333, 61202314, 61402371, 61402274), the Key Science and Technology Program of Shaanxi Province (Grant No. 2016GY-081), and Natural Science Basic Research Plan in Shaanxi Province of China (Grant No. 2015JM6317).

## References

- [1] H.M. Al-Otum, Morphological operators for color image processing based on Mahalanobis distance measure, *Opt. Eng.* 42 (9) (2003) 2595–2606.
- [2] H.M. Al-Otum, A novel set of image morphological operators using a modified vector distance measure with color pixel classification, *J. Visual Commun. Image Represent.* 30 (7) (2015) 46–63.
- [3] J. Angulo, Morphological colour operators in totally ordered lattices based on distance: application to image filtering, enhancement and analysis, *Comput. Vision Image Underst.* 107 (1–2) (2007) 56–73.
- [4] J. Angulo, Geometric algebra colour image representations and derived total orderings for morphological operators – part I: colour quaternions, *J. Vision Commun. Image Represent.* 21 (1) (2010) 33–48.
- [5] J. Angulo, Hypercomplex mathematical morphology, *J. Math. Imaging Vision* 41 (1–2) (2011) 86–108.
- [6] J. Angulo, Morphological bilateral filtering, *SIAM J. Imaging Sci.* 6 (3) (2013) 1790–1822.
- [7] E. Aptoula, S. Lefèvre, A comparative study on multivariate mathematical morphology, *Pattern Recognit.* 40 (11) (2007) 2914–2929.
- [8] E. Aptoula, S. Lefèvre, On lexicographical ordering in multivariate mathematical morphology, *Pattern Recognit. Lett.* 29 (2) (2008) 109–118.
- [9] E. Aptoula, S. Lefèvre,  $\alpha$ -Trimmed lexicographical extrema for pseudo-morphological image analysis, *J. Visual Commun. Image Represent.* 19 (3) (2008) 165–174.
- [10] J.C. Bezdek, R. Ehrlich, W. Full, FCM: The fuzzy c-means clustering algorithm, *Comput. Geosci.* 10 (2–3) (1984) 191–203.
- [11] N. Bouaynaya, M. Charif-Chechaouni, D. Schonfeld, Theoretical foundations of spatially-variant mathematical morphology part II: gray-level images, *IEEE Trans. Pattern Anal. Mach. Intell.* 30 (5) (2008) 837–850.
- [12] A. Căliman, M. Ivanovici, N. Richard, Probabilistic pseudo-morphology for grayscale and color images, *Pattern Recognit.* 47 (2) (2014) 721–735.
- [13] J.J. Chen, C.R. Su, W.E.L. Grimson, et al., Object segmentation of database images by dual multiscale morphological reconstructions and retrieval applications, *IEEE Trans. Image Process.* 21 (2) (2012) 828–843.
- [14] E. Chevallier, J. Angulo, The irregularity issue of total orders on metric spaces and its consequences for mathematical morphology, *J. Math. Imaging Vision* (2015) 1–14.
- [15] M. Dalla Mura, A. Villa, J.A. Benediktsson, et al., Classification of hyperspectral images by using extended morphological attribute profiles and independent component analysis, *IEEE Geosci. Remote Sens. Lett.* 8 (3) (2011) 542–546.
- [16] V. De Witte, S. Schulte, M. Nachtegael, et al., Vector morphological operators for colour images, in: LNCS, 3656, 2005, pp. 667–675.
- [17] M.G. Gong, Y. Liang, J. Shi, et al., Fuzzy c-means clustering with local information and kernel metric for image segmentation, *IEEE Trans. Image Process.* 22 (2) (2013) 573–584.
- [18] V. González-Castro, J. Debayle, J.C. Pinoli, Color adaptive neighborhood mathematical morphology and its application to pixel-level classification, *Pattern Recognit. Lett.* 47 (4) (2014) 50–62.
- [19] J. Goutsias, H.J.A.M. Heijmans, K. Sivakumar, Morphological operators for image sequences, *Comput. Vision Image Underst.* 62 (3) (1995) 326–346.
- [20] J.J. van de Gronde, J.B.T.M. Roerdink, in: Group-Invariant Frames for Colour Morphology, Mathematical Morphology and its Applications to Signal and Image Processing, 7883, Springer, Berlin, Heidelberg, 2013, pp. 267–278.
- [21] J.J. van de Gronde, J.B.T.M. Roerdink, Group-invariant colour morphology based on frames, *IEEE Trans. Image Process.* 23 (3) (2014) 1276–1288.
- [22] A. Hanbury, J. Serra, Mathematical morphology in the CIELAB space, *Image Anal. Stereol.* 21 (3) (2003) 201–206.
- [23] T.Y. Ji, Z. Lu, Q.H. Wu, Optimal soft morphological filter for periodic noise using a particle swarm optimizer with passive congregation, *Signal Process.* 87 (11) (2008) 2779–2809.
- [24] L. Jin, D. Li, E. Song, Combining vector ordering and spatial information for color image interpolation, *Image Vision Comput.* 27 (4) (2009) 410–416.
- [25] P. Kuosmanen, J. Astola, Soft morphological filtering, *J. Math. Imaging Vision* 5 (3) (1995) 231–262.
- [26] C. Kurtz, B. Naegel, N. Passat, Connected filtering based on multivalued component-trees, *IEEE Trans. Image Process.* 23 (12) (2014) 5152–5164.
- [27] S. Krinidis, V. Chatzis, A robust fuzzy local information C-means clustering algorithm, *IEEE Trans. Image Process.* 19 (5) (2010) 1328–1337.
- [28] T. Lei, Y.Y. Fan, Noise gradient reduction based on morphological dual operators, *IET Image Proc.* 5 (1) (2011) 1–17.
- [29] T. Lei, Y.Y. Fan, C.R. Zhang, X.P. Wang, Vector mathematical morphological operators based on fuzzy extremum estimation, in: IEEE International Conference on Image Processing, 2013, pp. 3031–3034.
- [30] T. Lei, Y. Wang, Y.Y. Fan, Vector morphological operators in HSV color space, *Sci. China Inf. Sci.* 56 (1) (2013) 1–12.
- [31] J. Li, Y. Li, Multivariate mathematical morphology based on principal component analysis: initial results in building extraction, in: The 20th ISPRS, 35, 2004, pp. 1168–1173.
- [32] W. Liao, R. Bellens, A. Pizurica, et al., Classification of hyperspectral data over urban areas using directional morphological profiles and semi-supervised feature extraction, *IEEE J. Sel. Topics Appl. Earth Obs. Remote Sens.* 5 (4) (2012) 1177–1190.
- [33] G. Licciardi, P.R. Marpu, J. Chanussot, et al., Linear versus nonlinear PCA for the classification of hyperspectral data based on the extended morphological profiles, *IEEE Geosci. Remote Sens. Lett.* 9 (3) (2012) 447–451.
- [34] G. Louverdis, I. Andreadis, P. Tsalides, New fuzzy model for morphological colour image processing, *IEE Proceedings-Vision, Image Signal Process.* 149 (3) (2002) 129–139.
- [35] G. Louverdis, M.I. Vardavoulia, I. Andreadis, P. Tsalides, A new approach to morphological color image processing, *Pattern Recognit.* 35 (8) (2002) 1733–1741.
- [36] P. Márquez-Neila, L. Baumela, L. Alvarez, A morphological approach to curvature-based evolution of curves and surfaces, *IEEE Trans. Pattern Anal. Mach. Intell.* 36 (1) (2014) 2–17.
- [37] L. Olivier, A. Elmoataz, Nonlocal and multivariate mathematical morphology, in: IEEE International Conference on Image Processing, 2012, pp. 129–132.
- [38] N. Passat, B. Naegel, Component-trees and multivalued image: structural properties, *J. Math. Imaging Vision* 49 (1) (2014) 37–50.
- [39] J. Serra, Introduction to mathematical morphology, *Comput. Vision Graphics Image Process.* 35 (3) (1986) 283–305.

- [40] J. Serra, Connectivity on complete lattices, *J. Math. Imaging Vision* 9 (3) (1998) 231–251.
- [41] M.I. Vardavoulia, I. Andreadis, P. Tsalides, Vector ordering and morphological operations for colour image processing: fundamentals and applications, *Pattern Anal. Appl.* 5 (3) (2002) 271–287.
- [42] S. Velasco-Forero, J. Angulo, Morphological processing of hyperspectral images using kriging-based supervised ordering, in: *IEEE International Conference on Image Processing*, 2010, pp. 1409–1412.
- [43] S. Velasco-Forero, J. Angulo, Mathematical morphology for vector images using statistical depth, *Math. Morphol. its Appl. Image Signal Process.* 6671 (2011) 355–366.
- [44] S. Velasco-Forero, J. Angulo, Supervised ordering in  $\mathbb{R}^P$ : application to morphological processing of hyperspectral images, *IEEE Trans. Image Process.* 20 (11) (2011) 3301–3308.
- [45] S. Velasco-Forero, J. Angulo, Random projection depth for multivariate mathematical morphology, *IEEE J. Sel. Topics Signal Process.* 6 (7) (2012) 753–763.
- [46] Z.X. Zhao, L.Z. Cheng, G.Q. Cheng, Neighbourhood weighted fuzzy c-means clustering algorithm for image segmentation, *IET Image Proc.* 8 (3) (2013) 150–161.